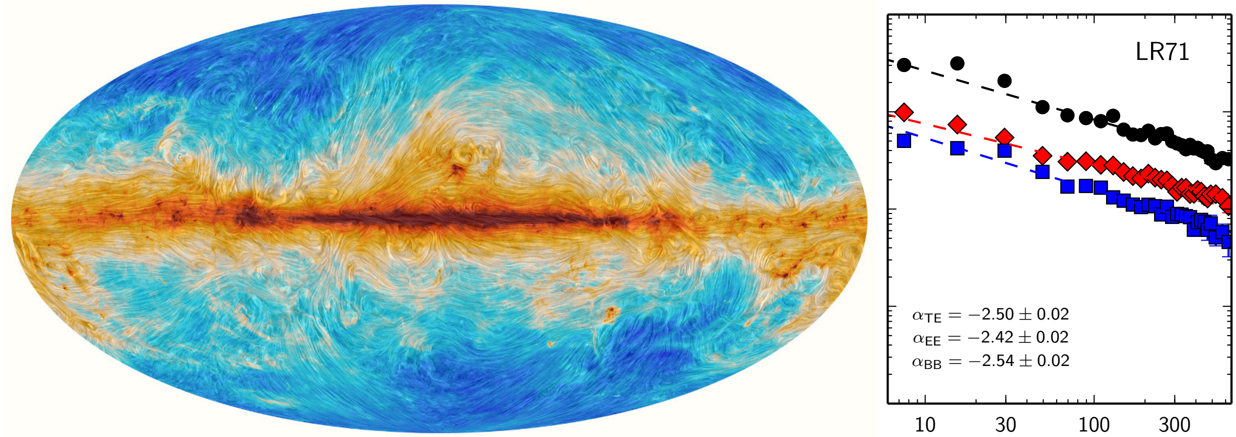

Figure 1: (*Left*) The *Planck* polarization map showing the 353 GHz dust intensity convolved with the direction of polarization (**?**). This shows coherent structure on a range of scales throughout the Milky Way. (*Right*) The spectrum of polarized emission from the sky, showing C_ℓ^{TT} in black, C_ℓ^{EE} in red, and C_ℓ^{BB} in blue.

The Dust Between Us and the Big Bang

PI: David C. Collins (Florida State University)

We are requesting 8.0×10^6 core-hours on the Anvil supercomputer and 1.8×10^5Gb on the Ranch archival system in order to perform several simulations. These simulations are in support of a campaign to observe gravitational waves from the Big Bang.

Table 1: Summary of SU and disk request for two suites of simulations, and disk to accommodate our existing archive

	SU	Disk
Galaxies	5.0×10^6	5.3×10^3 Gb
Turbulence	3.0×10^6	1.6×10^3 Gb
Analysis	2.6×10^5	–
Archive	–	1.7×10^5 Gb
	8.0×10^6	1.8×10^5 Gb

The cosmic microwave background (CMB) contains the oldest light in the universe, having been emitted 400,000 yr after the Big Bang. The CMB has been well studied, and it has taught us many things about the size, age, expansion, and contents of the Universe. To learn more, we must look at its polarization. The polarization of the CMB contains an imprint of gravitational waves launched at the Big Bang, which will answer more questions about the beginning of the Universe. Unfortunately, the dust and plasma in the interstellar medium (ISM) of our own Milky Way Galaxy produces a polarized signal that is much brighter than the CMB in similar frequencies. In order to see the primordial polarization, we must first understand our Galactic polarization. We will perform simulations in order to understand the nature of this signal. In the future we will work to remove it from future CMB experiments such as CMB S4 and Simons Observatory. We will perform two suites of simulations; the suite of driven *turbulence* will analyze small scale features, and the second is a suite of full *galaxy* simulations that will cover the large scale and parity violating signals.

We have been awarded 2×10^5 SU (Node-hours) on *Frontera* to do two large scale turbulence simulations and three large scale galaxy simulations. The proposed simulations compliment these by covering more parameter space, which is necessary for making predictions, at a lower resolution. Taken together we hope to make useful predictions about the polarization signature of the interstellar medium.

1 Scientific Background

The Planck satellite measured the microwave polarization over the whole sky (Planck Collaboration et al. 2020). Figure 1 shows an image of the magnetic field implied by these polarizations (left panel). In this image, the color indicates the total dust emission, and the image has been smoothed along the direction of the magneticfield. In the

ISM, polarization in the microwave is caused by thermal emission from dust that is lined up along the magnetic field, like iron filings. Additionally, hot synchrotron electrons also emit in the microwave, and are also polarized by the magnetic field. These synchrotron electrons occupy a different part of the galaxy than the dust due to their higher temperature, and therefore scale height.

Since polarization is a vector in the plane of the sky, in order to quantitatively describe it one needs two fields. Often Stokes parameters, Q and U are used, but these are coordinate dependent quantities, and Q rotates into U as the telescope rotates. It is better to use E and B, which are the parity-even and parity-odd combinations of Q and U. Roughly, E describes polarization parallel and perpendicular to filamentary structure that dominates the ISM, and B describes polarization oblique to filaments. The spectral signal, of E, B, and total emission T can be seen in the right panel of Figure 1. It is found that the emission is distributed as a power law, with spectral slopes of T, E, and B all roughly -2.5. This can be seen in the left panel of Figure 1, which shows spectral power of T, E and B vs. wavenumber, ℓ.

The correlations between T, E and B are also of interest. The TB correlation was found by Planck (Planck Collaboration et al. 2020) to be statistically significant with a correlation coefficient of $r_{TB} = 0.05$. This is counter-intuitive, as the total emission should be parity even, but B is parity odd, so the mean of their correlation should be zero. This indicates a large scale structure in the galaxy (Brandenburg & Brüggen 2020), or some kind of handedness to the filamentary structures in the ISM (Huffenberger et al. 2020).

In our preliminary work, to appear soon as Stalpes et al (2024, in prep), we simulated clouds of plasma in the ISM as periodic boxes of supersonically turbulent fluid. Simulations of driven turbulence were performed, wherein kinetic energy is added to the gas at the large scale, and then cascades to smaller and smaller scales, until the dissipation scale is reached. We did this for a range of sonic and Alfvén Mach numbers. The sonic Mach number is defined as $\mathcal{M} = v/c$, where v is the r.m.s velocity and c is the speed of sound, while the Alfvén Mach number, $\mathcal{M}_{\mathrm{A}} = v/v_A$, where v_A is the Alfvén speed, the typical speed for magnetic waves. Increasing the kinetic energy (increasing $\mathcal{M}$) of the cloud creates smaller structures, while increasing magnetic field strength (decreasing Alfvén) suppresses small structure. Our simulations were performed at a modest resolution of 512^3. We found, from synthetic observations of the boxes, that the spectral slope of T, E and B are all reproduced for a ($\mathcal{M}$, $\mathcal{M}_{\mathrm{A}}$)=(4.7, 1.5). This is an over simplification, as the true ISM exhibits a range of properties, but a useful benchmark for future study. We do not, however, find that the TB correlations are as large as those found on the sky. This implies that there is likely a large scale structure in the T, E and B signals, that comes from the shape of the magnetic field as it is wound around the galaxy.

To this end, we are also exploring the polarization signature of full galaxy simulations that include not only the disk of the galaxy, but the circumgalactic medium (CGM) that surrounds the galaxy. By simulating the full galaxy and a large spatial extent, we will capture the boundary conditions of the nearby (close to the midplane) magnetic structures as well as the higher latitude structures to capture the synchrotron signature. The galactic simulations proposed here aim to explore the nature of the CGM and its connection to the ISM, as well as the growth and distribution of the magnetic field around the galaxy.

One of the challenges in understanding the polarization of the CMB foregrounds is the small spatial scales necessary, as the signal of primordial gravitational waves lives at the sub-degree scale, as well as the large scale spatial modes to capture the non-trivial TB correlation, within the general chaos of a galaxy. Our multi-tier approach is essential for covering the range of parameter space the Milky Way exhibits, and the spatial resolution ultimately necessary to make meaningful predictions of the foregrounds of the polarized CMB. The simulations proposed here (12 simulations of driven turbulence at 1024^3 and 9 galactic simulations with a midplane resolution of 12pc) compliment each other in that they capture both small and large scale features over the range of parameters likely to be experienced by the ISM. This also compliments our *Frontera* allocation, which covers an extremely limited parameter space in exchange for very high resolution. The simulations presented here will ensure success of the high resolution simulations. In addition, the outstanding memory capacity of *Anvil* will be a great boon in analyzing the large simulations from the *Frontera* allocation.

The ultimate goal is to simulate an entire galaxy with 1 pc resolution. Our proposed galaxy simulations are an AMR stack with approximately 256^3 zones per level for 8 levels, with an outer box size of 8192pc and a finest resolution of 12.5 pc. The *Frontera* simulations double the resolution at every level and achieve 6.25pc resolution. Once we are successful with these simulations, we will extend to 1024^3 per level for 8 levels, which will get 3.125pc resolution at the midplane of the galaxy. We will ultimately combine the knowledge gained from our 2048^3 simulations, the simulations of our 512^3 tower, and the experience and preliminary science gained in the currently proposed simulations to launch simulations of galaxies at 1pc resolution at the midplane.

We describe the code to be used in Section 2. A detailed description of the simulations to be performed is in Section 3, and the detailed accounting of the disk and SU request is in Section 4. The interaction with the other allocation in Section 5.

2 Methods

The code we will use is Enzo (Bryan et al. 2014; Collins et al. 2010), an open source code that has been used for a number of astrophysics applications (e.g. Abel et al. 2002; Correa Magnus et al. 2023). Enzo is an adaptive mesh refinement (AMR) code that can dynamically add resolution elements as the system requires it, using the strategy of Berger & Colella (1989) and Balsara (2001). We will use the constrained transport (CT) module (Collins et al. 2010; Gardiner & Stone 2005) that conserves the divergence of the field to machine precision. It uses FFT-based gravity for the root grid and multigrid relaxation for gravity on fine grids. The base MHD solver is a higher order Godunov method. We will use Grackle (Smith et al. 2017) to handle the chemistry and thermodynamics.

3 Simulations

Our proposed simulations are in two suites. The first suite is 12 simulations of driven turbulence. These simulations, while highly idealized, will examine the detailed relation between the state of the ISM and its contribution to polarization foregrounds. The second suite is 9 full galaxy simulations. These lack resolution, but will serve as preliminary runs to ensure the initial conditions and subgrid models will behave at scale before performing the larger scale simulations. We additionally propose time for analysis of both allocations

3.1 Turbulence Simulations

The ISM is dominated by turbulence, and driven turbulent boxes are the most efficient way to separate driving scale and dissipation scale in spectral space to simulate turbulence in a self consistent way. The driving scale is a boundary condition provided by the scientist, and the dissipation scale is a combination of resolution and method. Increasing resolution increases the separation between these boundary conditions and allow us to explore the true nonlinear physics of fluid dynamics. The preliminary simulations of Stalpes et al showed power law behavior of E and B with appropriate slopes, but only in a limited range of spectral space, in some cases negligible. Further, we were unable to proceed to Mach numbers higher than 6 due to the limited spatial resolution. High Mach number simulations result in large density contrast, which is equivalent to high spatial contrast, which is only realizable with high resolution. In Stalpes et al, we predict that the typical Mach and Alfvén Mach numbers are 4.7 and 1.5. Our high resolution simulations target this parameter space. But thee true ISM is multiphase, with many patches exhibiting a wide range of temperatures, densities, sound speeds, and Mach numbers. Thus we also propose a suite of 12 simulations, where we verify the results of Stalpes et al, as well as extending to higher Mach numbers, and anticipating the success of our *Frontera* simulations.

We will simulate for 5 dynamical times FLESH THIS OUT

Table 2: Detailed accounting for each suite of simulations. The galaxy simulations are broken down by level for one galaxy. $N_Z = 1.1 \times 10^9$ for the turbulence simulations. We will use 512 cores for the galaxy simulations and 4096 cores for the turbulence simulations, using the whole node (128 cores) for all simulations.

suite	ℓ	N_Z	ΔT[s]	dT[s]	ζ	SU
Galaxy	8	4.1×10^7	3.1×10^{10}	6.3×10^{16}	5.0×10^4	4.7×10^5
Galaxy	7	3.6×10^7	6.2×10^{10}	6.3×10^{16}	5.0×10^4	2.0×10^5
Galaxy	6	4.1×10^7	1.2×10^{11}	6.3×10^{16}	5.0×10^4	1.2×10^5
Galaxy	5	1.7×10^7	2.5×10^{11}	6.3×10^{16}	5.0×10^4	2.4×10^4
Galaxy	4	1.7×10^7	4.9×10^{11}	6.3×10^{16}	5.0×10^4	1.2×10^4
Galaxy	3	1.7×10^7	9.9×10^{11}	6.3×10^{16}	5.0×10^4	6.0×10^3
Galaxy	2	1.7×10^7	2.0×10^{12}	6.3×10^{16}	5.0×10^4	3.0×10^3
Galaxy	1	1.7×10^7	3.9×10^{12}	6.3×10^{16}	5.0×10^4	1.5×10^3
Galaxy	0	1.7×10^7	7.9×10^{12}	6.3×10^{16}	5.0×10^4	7.4×10^2
				Total SU	1 galaxy	8.3×10^5
				Total Disk	1 galaxy	8.8×10^2
				Total SU	**6 galaxies**	5.0×10^6
				Total Disk	**6 galaxies**	5.3×10^3
suite	$\mathcal{M}$	$\mathcal{M}_{\rm A}$	ΔT	dT	ζ	SU
Turbulence	2	0.75	1.3	3.3×10^{-6}	2.4×10^5	4.7×10^5
Turbulence	2	1.5	1.3	4.4×10^{-6}	2.4×10^5	3.6×10^5
Turbulence	2	3	1.3	5.2×10^{-6}	2.4×10^5	3.0×10^5
Turbulence	4.7	0.75	0.5	1.6×10^{-6}	2.4×10^5	4.2×10^5
Turbulence	4.7	1.5	0.5	2.1×10^{-6}	2.4×10^5	3.1×10^5
Turbulence	4.7	3	0.5	2.6×10^{-6}	2.4×10^5	2.5×10^5
Turbulence	8	0.75	0.3	9.6×10^{-7}	2.4×10^5	4.0×10^5
Turbulence	8	1.5	0.3	1.3×10^{-6}	2.4×10^5	2.9×10^5
Turbulence	8	3	0.3	1.6×10^{-6}	2.4×10^5	2.4×10^5
Turbulence	12	0.75	0.3	6.5×10^{-7}	2.4×10^5	4.8×10^5
Turbulence	12	1.5	0.2	9.0×10^{-7}	2.4×10^5	2.9×10^5
Turbulence	12	3	0.2	1.1×10^{-6}	2.4×10^5	2.3×10^5
					Total SU	3.0×10^6
					Total Disk	1.6×10^3

3.2 Galaxy Simulations

Our ultimate desire is to simulate the mid-plane of a galaxy with 1pc resolution while also simulating the CGM to roughy 1Mpc. This will give us a realistic picture of the small scale CMB foregrounds where the interesting signal lies, as well as the large scale properties that are necessary for its removal. This will proceed in several steps.

MORE FLESH SHIT I DIDNT FINISH

4 Request Details

The cost for each simulation is found as

$$SU = t_{wall} N_C \tag{1}$$

$$t_{wall} = \frac{\sum_\ell N_Z N_U}{\zeta} \frac{1}{N_C}, \tag{2}$$

where SU is the total cost in core-hours; t_{wall} is the run time; N_Z is the number of zones per level ℓ; N_U is the number of updates per level; ζ is the performance measured in (zone-updates)/(processor-second); and N_C is the total number of cores. The cost, $zeta$, is determined in the scaling document. Total disk usage is found as

$$Disk = 8 N_Z N_F N_D \text{bytes}, \tag{3}$$

where each of N_Z zones contains N_F fields and we store N_D dumps for each run. The values of N_N, N_C, N_F, N_D and ζ can be found in N_F = (20, 27) and N_D=(10,20) for the (turbulence, galaxy) simulations, respectively. The values of N_Z and N_U are outlined in Table 2 and the rest of this section.

The number of zones, N_Z, is computed from the problem geometry. All of these simulations will use fixed or static resolution, so N_Z is known. For the *turbulence* simulations, $N_Z = 1024^3$. For the galaxy simulations, N_Z will be computed level-by-level from the grid layout. We construct each level in grid patches of 32^3 zones each. Consistent patch size allows us to optimize the memory usage and performance of the simulation. The finest level is a thin pancake of $100 \times 100 \times 1$ grids. This covers the midplane with a resolution of 12.5 pc for the entire disk, to the dust scale height of ± 100pc and a side length of 20kpc. Resolution increases by a factor of 2 each level. The next two levels increase the aspect ratio of the refined region ($54 \times 54 \times 3$ and $30 \times 30 \times 11$ grids, respectively), and the remaining levels are $16 \times 16 \times 16$ grids. This grid structure gives an outer size of 8.2×10^5pc on a side with 12.5pc resolution over the whole disk at the midplane.

The number of updates is found from the total simulation time over the step size, $N_U = \Delta T/dt$. T by the problem goals, and we estimate dt from the solver behavior and prior results. As described above, the *turbulence* simulations will run for $T = 5t_{dyn} = 5/(2\mathcal{M})$ (in dimensionless code units), to statistically resolve the turbulence. The *galaxy* simulations will run for $T = 2$ Gyr, which represents roughly 8 orbits of the galaxy, hopefully enough time to grow the magnetic field. The timestep size, dt, is found by a standard Courant condition,

$$\Delta t = \eta \frac{\Delta x}{(v + c_f)_{max}}, \tag{4}$$

where $(v + c_f)_{max}$ is the maximum signal velocity on each resolution level. Here, v is the velocity and c_f is the fast MHD speed. It is not possible to predict the exact value of this signal speed, so we calibrate to lower resolution simulations and use Equation 4 to rescale. For the *turbulence* simulations, we calibrate Δt to the fiducial simulations in Stalpes et al (2023). For the *galaxy* simulations, we calibrate to a low-resolution preliminary galaxy.

Table 2 shows a summary of the request. The first porton show each level of one *galaxy* simulation, estimating N_Z and $N_U = \Delta T/dt$ and the total cost, SU, for each level ℓ. The second portion shows the cost for each turbulence simulation, broken down by Mach numbers which dictate both ΔT and dt.

5 Access to Other Resources

In addition to our existing Access-Maximize allocation, our team recently secured $2{\times}10^5$ node-hours on *Frontera* by way of a *Pathways* allocation. The *Frontera* allocation will be used to run the high resolution counterparts to this study. This includes two turbulence simulations at 2048^3 and three galaxies with roughly 512^3 zones per level. These mirror the proposed simulations in form, but are a factor of 8 larger in memory and a factor of 16 more expensive in SUs. Thus the *Anvil* simulations will serve to cover parameter space, while the *Frontera* simulations target specific configurations with high resolution. Both are necessary in our quest for a complete picture of magnetic fields in our Galaxy. The *Frontera* allocation cannot be also used for these simulations as the high resolution (2048^3 for the turbulence runs and 8 levels of 512^3 for the galaxy runs) are quite expensive and will require the whole allocation.

References

Abel, T., Bryan, G. L., & Norman, M. L. 2002, Science, 295, 93

Balsara, D. S. 2001, J. Comput. Phys, 174, 614

Berger, M. J. & Colella, P. 1989, J. Comput. Phys, 82, 64

Brandenburg, A. & Brüggen, M. 2020, ApJ, 896, L14

Bryan, G. L., Norman, M. L., O'Shea, B. W., Abel, T., Wise, J. H., Turk, M. J., Reynolds, D. R., Collins, D. C., Wang, P., Skillman, S. W., Smith, B., Harkness, R. P., Bordner, J., Kim, J.-h., Kuhlen, M., Xu, H., Goldbaum, N., Hummels, C., Kritsuk, A. G., Tasker, E., Skory, S., Simpson, C. M., Hahn, O., Oishi, J. S., So, G. C., Zhao, F., Cen, R., Li, Y., & Enzo Collaboration. 2014, ApJS, 211, 19

Collins, D. C., Xu, H., Norman, M. L., Li, H., & Li, S. 2010, ApJS, 186, 308

Correa Magnus, L., Smith, B. D., Khochfar, S., O'Shea, B. W., Wise, J. H., Norman, M. L., & Turk, M. J. 2023, arXiv e-prints, arXiv:2307.03521

Gardiner, T. A. & Stone, J. M. 2005, J. Comput. Phys, 205, 509

Huffenberger, K. M., Rotti, A., & Collins, D. C. 2020, ApJ, 899, 31

Planck Collaboration, Akrami, Y., Ashdown, M., Aumont, J., Baccigalupi, C., Ballardini, M., Banday, A. J., Barreiro, R. B., Bartolo, N., Basak, S., Benabed, K., Bernard, J. P., Bersanelli, M., Bielewicz, P., Bond, J. R., Borrill, J., Bouchet, F. R., Boulanger, F., Bracco, A., Bucher, M., Burigana, C., Calabrese, E., Cardoso, J. F., Carron, J., Chiang, H. C., Combet, C., Crill, B. P., de Bernardis, P., de Zotti, G., Delabrouille, J., Delouis, J. M., Di Valentino, E., Dickinson, C., Diego, J. M., Ducout, A., Dupac, X., Efstathiou, G., Elsner, F., Enßlin, T. A., Falgarone, E., Fantaye, Y., Ferrière, K., Finelli, F., Forastieri, F., Frailis, M., Fraisse, A. A., Franceschi, E., Frolov, A., Galeotta, S., Galli, S., Ganga, K., Génova-Santos, R. T., Ghosh, T., González-Nuevo, J., Górski, K. M., Gruppuso, A., Gudmundsson, J. E., Guillet, V., Handley, W., Hansen, F. K., Herranz, D., Huang, Z., Jaffe, A. H., Jones, W. C., Keihänen, E., Keskitalo, R., Kiiveri, K., Kim, J., Krachmalnicoff, N., Kunz, M., Kurki-Suonio, H., Lamarre, J. M., Lasenby, A., Le Jeune, M., Levrier, F., Liguori, M., Lilje, P. B., Lindholm, V., López-Caniego, M., Lubin, P. M., Ma, Y. Z., Macías-Pérez, J. F., Maggio, G., Maino, D., Mandolesi, N., Mangilli, A., Martin, P. G., Martínez-González, E., Matarrese, S., McEwen, J. D., Meinhold, P. R., Melchiorri, A., Migliaccio, M., Miville-Deschênes, M. A., Molinari, D., Moneti, A., Montier, L., Morgante, G., Natoli, P., Pagano, L., Paoletti, D., Pettorino, V., Piacentini, F., Polenta, G., Puget, J. L., Rachen, J. P., Reinecke, M., Remazeilles, M., Renzi, A., Rocha, G., Rosset, C., Roudier, G., Rubiño-Martín, J. A., Ruiz-Granados, B., Salvati, L., Sandri, M., Savelainen, M., Scott, D., Soler, J. D., Spencer, L. D., Tauber, J. A., Tavagnacco, D., Toffolatti, L., Tomasi, M., Trombetti, T., Valiviita, J., Vansyngel, F., Van Tent, B., Vielva, P., Villa, F., Vittorio, N., Wehus, I. K., Zacchei, A., & Zonca, A. 2020, A&A, 641, A11

Smith, B. D., Bryan, G. L., Glover, S. C. O., Goldbaum, N. J., Turk, M. J., Regan, J., Wise, J. H., Schive, H.-Y., Abel, T., Emerick, A., O'Shea, B. W., Anninos, P., Hummels, C. B., & Khochfar, S. 2017, MNRAS, 466, 2217